Critical Parameters for Heat Transfer and Chemical Reactions in Thermosetting Materials

B. RIKARD GEBART

Swedish Institute of Composites, Box 271, S-941 26 Piteå, Sweden

SYNOPSIS

The equations of one-dimensional heat transfer with chemical reactions with isothermal initial conditions and constant wall temperature are solved approximately for all types of kinetic models. The general solution is valid for low exothermal peaks and it is characterized explicitly by two dimensionless parameters. The first parameter is the ratio between the time scale for heat conduction and that for the chemical reaction; the second parameter is the ratio between the processing temperature and the adiabatic temperature rise. The number of additional parameters depends on the particular choice of kinetic model. The maximum temperature in the solution always occur at the center line and its magnitude is proportional to the maximum rate of reaction. For a second-order autocatalytic kinetic model, closed form results can be obtained. The solution is in this case characterized by two additional dimensionless parameters. The analytical solution agrees excellently with numerical solutions for small exothermal temperature peaks ($< 10\%$ of the adiabatic temperature rise), but the qualitative agreement is very good also for cases with significant exothermal peaks. The general solution can be used also for the case when the kinetic model is unknown and only experimental DSC results are available. © 1994 John Wiley & Sons, Inc.

INTRODUCTION

The quality of fiber-reinforced composite parts made with thermoset resins depends to a large extent on the curing process. The temperature in the laminate must be kept as uniform as possible during cure to avoid residual stresses after cooling. Moreover, thermal degradation of the matrix or voids from gas formed by chemical reactions may occur if the maximum temperature in the laminate becomes too high. This may sometimes be in conflict with the demand for short cycle times, which often necessitates high processing temperatures that may give strong temperature gradients.

Nonuniform and high temperature usually occurs when the laminate is thick in some sense. A strict definition of a thick laminate is difficult to make since it depends both on the reactivity of the thermoset at the processing temperature and the thermal properties of the laminate (heat conductivity, specific heat capacity, and density). One way to estimate when a laminate can be considered "thick" is to compute the ratio between the time scale for the reaction and the time scale for heat conduction. Adiabatic behavior with high temperatures can be expected when this ratio is much less than unity.[1]

Several kinetic models have been proposed for use in the simulation of the cure process in thermosetting materials. The most complex models are based on a semimechanistic approach.[2,3] However, these models are usually quite impractical for engineering purposes due to the difficulty in obtaining the model parameters. An alternative to the fundamental models are empirical or phenomenological models formulated in terms of the degree of cure (or the degree of conversion), which are much easier to apply in a practical case. The degree of cure can be defined as[4]

$$\alpha(t) = \frac{\int_0^t q_r(t')\,dt'}{\rho H_{\text{tot}}} \tag{1}$$

where q_r is the heat production per unit mass by chemical reactions; ρ, the density of the composite, and H_{tot}, the total amount of heat that is released per unit mass if the reaction is allowed to progress until completion. The simplest model of this kind is the so-called nth-order kinetic model,[1,5] which describes how the rate of reaction depends on the degree of cure and the temperature:

$$\frac{d\alpha}{dt} = K(1 - \alpha)^n \qquad (2)$$

where K is a temperature-dependent parameter usually described by an Arrhenius expression. This model can be slightly refined to take account of diffusion controlled phenomena[6] by substituting a temperature-dependent function α_{max} inside the parentheses:

$$\frac{d\alpha}{dt} = K(\alpha_{max} - \alpha)^n \qquad (3)$$

Both models (2) and (3) are unable to model the maximum in the rate of reaction for intermediate values of α that is observed for autocatalytic materials. A model that can describe autocatalytic behavior was proposed by Kamal and Sourour[7-9]:

$$\frac{d\alpha}{dt} = (K_1 + K_2\alpha^m)(1 - \alpha)^n \qquad (4)$$

where K_1 and K_2 are temperature-dependent parameters. An alternative form of (4) with $K_1 = 0$ has been found to work well for unsaturated polyesters.[10] Measurements in our own lab show that (4) with $K_1 = 0$ works reasonably well also for epoxy and vinylester. The model in (4) can be refined in a similar way to the nth-order model to take account of diffusion-controlled behavior at the later stages of the reaction[11] to yield

$$\frac{d\alpha}{dt} = (K_1 + K_2\alpha^m)(\alpha_{max} - \alpha)^n \qquad (5)$$

where α_{max} is a linear function of temperature.

In the present study, an explicit solution is presented for temperature and chemical reactions characterized by the autocatalytic model in (4) with $m + n = 2$ (second-order reaction) and with $K_1 = 0$:

$$\frac{d\alpha}{dt} = K_2\alpha^{2-n}(1 - \alpha)^n \qquad (6)$$

which is sufficient to model the important features of many real materials (see Fig. 1). The purpose of the present article was to investigate the influence on the temperature and the cure time for different process parameters. The simple model in (6) exhibits most of the important features of the more refined models. The main limitation is the poor description of the ultimate degree of cure at different temperatures, but this has no practical importance for the exothermal temperature prediction and for the time to, say, 50% conversion. The dashed lines in Figure 1 are computed from a best fit of the model in (5) and the solid lines are from a best fit to the model in (6). Both models agree qualitatively well with the data, but the model in (5) agrees more closely quantitatively with the data, which is not so surprising since a larger number of fitting parameters usually gives a better fit. However, it is debatable whether the more complex model in (5) will give a better prediction of a real processing situation than will the other models, since the model parameters are difficult to determine with high accuracy (particularly K_1) and since it is very difficult to ensure that the processing conditions are exactly as in the theory.

The boundary and initial conditions for the energy equation has been investigated for different composite manufacturing processes by Castro.[12] The analysis of chemical reactions and the mold-filling process can be decoupled for cases where the mold filling time is much shorter than the gel time of the material. Castro also showed that the mold-filling process can be considered isothermal at the mold wall temperature if the time scale for heat conduction is much smaller than the time scale for the reaction. In the case of liquid composite molding processes such as structural reaction injection molding (SRIM) and resin transfer molding (RTM), the mold temperature is usually close to the initial temperature of the resin. In summary, this makes it reasonable to assume, in many processing situations, that the resin temperature is isothermal and at the mold temperature when the cure process starts.

For the case with high-speed liquid composite molding at higher temperatures and with minimized cure times, the case is not so clear and more work is needed to determine if an analysis with isothermal initial conditions at the mold temperature is feasible.

In this article, a general solution valid for small exotherm temperatures is developed. The general solution is specialized to the kinetic model in (6) so that an explicit analytical solution is obtained. The analytical solution is compared to a numerical solution of the full nonlinear problem and is found to
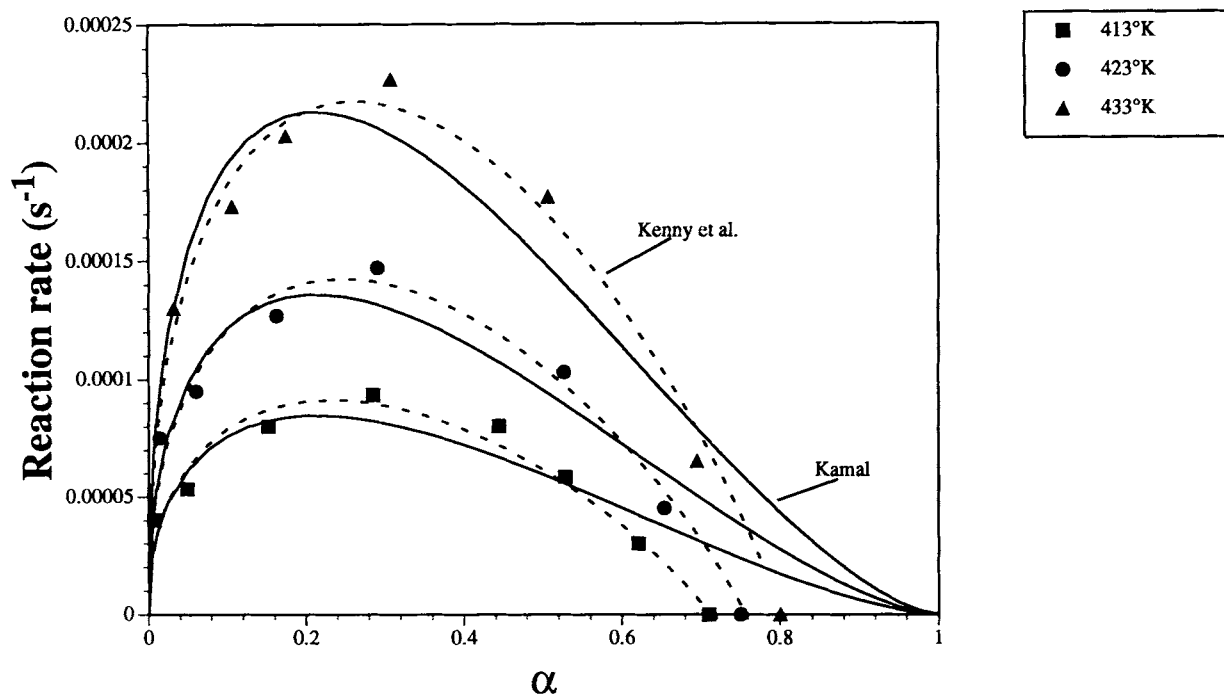
Figure 1   Comparison of the ability of two different kinetic models to describe the cure process for an epoxy resin (experimental data from Dusi et al.[9]). The solid line is a best fit to a simple second-order autocatalytic model and the dashed line is a fit to the model proposed by Kenny et al.[11] with $K_1 = 0$.

give good results for small exotherm temperatures. For higher exotherm temperature peaks, the model still gives qualitatively correct results. The big advantage with the analytical solution is that it gives a detailed "map" over the dependence on the problem parameters in contrast to the pointwise information that usually results from a numerical solution.

GENERAL SOLUTION FOR SMALL EXOTHERMAL PEAK TEMPERATURES

The following analysis is valid for a geometry in which the thickness is small compared with the width so that heat conduction is essentially one-dimensional. Moreover, the material properties are assumed to be independent of the temperature and the degree of cure. The equation for one-dimensional heat conduction with chemical reactions in a material with constant properties is[13]

$$\rho c \, \frac{\partial T}{\partial t} = \lambda \, \frac{\partial^2 T}{\partial x^2} + q_r \qquad (7)$$

where ρ is the density; c, the specific heat capacity; λ, the heat conductivity; and q_r, the heat production by chemical reactions. An equivalent expression for the heat production associated with the reactions can be derived from the definition of α in (1):

$$q_r = \rho H_{\text{tot}} \, \frac{d\alpha}{dt} \qquad (8)$$

The rate of reaction $d\alpha/dt$ is at this stage assumed to be described by the general expression

$$\frac{d\alpha}{dt} = f(\alpha, T) \qquad (9)$$

In the next section, a particular model will be used in place of the right-hand side of (9), but the analysis can be taken several steps forward without any further assumptions about the kinetic model. The boundary and initial conditions for the problem are

$$T = T_0; \quad \begin{cases} x = 0 \\ x = h \end{cases} \qquad (10)$$

$$\left. \begin{array}{c} T = T_0 \\ \\ \alpha = \varepsilon \end{array} \right\} \; ; \quad t = 0 \qquad (11)$$

The time scale for this problem depends primarily on the reactivity of the material and a suitable time scale can be derived from the reaction with adiabatic conditions for a small sample of material (small enough to be isothermal). For this case, the energy equation can be integrated directly to

$$T - T_0 = \frac{H_{tot}}{c} \alpha \qquad (12)$$

Substitution of T from (12) in the kinetic model Eq. (9) yields the reaction rate at different degrees of cure. The particular value of the degree of cure, denoted α_1 in the following, that is chosen to compute the characteristic rate of reaction should ideally be chosen so that $d\alpha/dt$ is at its maximum. However, for an order of magnitude estimate, any value of α in the interior of the interval $[0, 1]$ is acceptable. Thus, the characteristic value of the rate of reaction is

$$\frac{d\alpha}{dt}\bigg|_{char} = f(\alpha, T); \quad \left\{ \begin{array}{l} \alpha = \alpha_1 \\ \\ T = T_0 + \frac{H_{tot}}{c} \alpha_1 \end{array} \right. \qquad (13)$$

The time scale τ for a significant change of the degree of cure is the inverse of the characteristic rate of reaction:

$$\tau = \left[\frac{d\alpha}{dt}\bigg|_{char} \right]^{-1} \qquad (14)$$

The characteristic length scale of the problem is the thickness of the laminate L and a characteristic temperature is obtained from the adiabatic temperature rise ΔT_{ad}:

$$\Delta T_{ad} = \frac{H_{tot}}{c} \qquad (15)$$

The maximum change in temperature with the temperature normalized with ΔT_{ad} will be of order unity or smaller. However, higher temperature changes are possible if the boundary temperature is higher than T_0.[14,15] The degree of cure, α, needs no scaling since it is already dimensionless and of order unity by definition. Dimensionless variables are obtained by scaling of the original variables:

$$t^* = \frac{t}{\tau} \qquad (16)$$

$$\eta = \frac{x}{L} \qquad (17)$$

$$\theta = \frac{T}{\Delta T_{ad}} \qquad (18)$$

Substitution of these variables in the governing equations yields

$$\frac{\partial \theta}{\partial t^*} = \Omega \frac{\partial^2 \theta}{\partial \eta^2} + \frac{d\alpha}{dt^*} \qquad (19)$$

$$\frac{d\alpha}{dt^*} = F(\alpha, \theta) \qquad (20)$$

where the dimensionless kinetic model $F(\alpha, \theta)$ is defined by

$$F(\alpha, \theta) = \tau^{-1} f(\alpha, T); \quad T = \Delta T_{ad}\theta \qquad (21)$$

The dimensionless initial and boundary conditions are

$$\theta = \theta_0; \quad \left\{ \begin{array}{l} \eta = 0 \\ \\ \eta = 1 \end{array} \right. \qquad (22)$$

$$\left. \begin{array}{c} \theta = \theta_0 \\ \\ \alpha = \varepsilon \end{array} \right\} \; ; \quad t^* = 0 \qquad (23)$$

The two dimensionless parameters Ω and θ_0 are defined as

$$\Omega = \frac{\lambda \tau}{\rho c L^2} \qquad (24)$$

$$\theta_0 = \frac{T_0}{\Delta T_{ad}} \qquad (25)$$

The dimensionless kinetic model eq. (21) contains additional dimensionless parameters that depend on the particular model in question. The first dimensionless parameter Ω can be interpreted as the ratio of the time scale for the reaction to the time scale for heat conduction. It is sometimes called a diffusion Deborah number.[11] The second parameter θ_0 is the nondimensional initial temperature.

The dimensionless equations for the cure process [(19) and (20)] can be solved for the special case with close to isothermal conditions, which is obtained when the exothermal peak temperature is

small. In this case, the temperature variation is so small that the reaction rate is essentially the same as it is under isothermal conditions. This means that the energy equation and the kinetic equation become decoupled and can be solved in sequence. The kinetic equation can be integrated to

$$\alpha = G(\theta_0, t^*) \qquad (26)$$

where G is a time-dependent function that also depends on the parameter θ_0. It is difficult to find analytical expressions for G for most of the kinetic models presented in the Introduction. However, it is always possible to perform this step for any sensible kinetic model, although in some cases it is necessary to resort to a numerical solution. The solution for α yields a time-dependent solution for $d\alpha/dt$ independent of the temperature variation around θ_0:

$$\frac{d\alpha}{dt} = F_0(t^*) \qquad (27)$$

where F_0 is given by

$$F_0 = F[G(\theta_0, t^*), \theta_0] \qquad (28)$$

Notice that the solution in (26) and (27) can also be obtained directly from an isothermal DSC experiment. The DSC instrument can then be said to act as an analog computer. The solution for $d\alpha/dt$ in (27) is now substituted in place of the source term in (19). The general solution to (19) with the time-dependent energy source $F_0(t^*)$ from (27) is then[13]

$$\theta - \theta_0 = \frac{4}{\pi} \sum_{n=0}^{\infty} \frac{(-1)^n}{(2n+1)} \cos[(2n+1)\pi(\eta - 1/2)]$$

$$\times \int_0^{t^*} F_0(\tau) e^{-\Omega(2n+1)^2\pi^2(t^*-\tau)} \, d\tau \qquad (29)$$

The solution is valid for all values of Ω and all types of time-dependent source terms $F_0(t^*)$. The only assumption is that the resulting exotherm temperature peak must be so small that the kinetic and the energy equation are effectively uncoupled. The solution in (29) can be considerably simplified if the integral in the sum is solved approximately with Laplace's method[16]:

$$\theta - \theta_0 = \frac{4}{\pi} \sum_{n=0}^{\infty} \frac{(-1)^n}{(2n+1)} \cos[(2n+1)\pi(\eta - \tfrac{1}{2})]$$

$$\times F_0(t^*) \frac{1}{\Omega(2n+1)^2\pi^2} \qquad (30)$$

The result in (30) can be simplified even further since the sum can be evaluated explicitly to

$$\theta - \theta_0 = \frac{1}{2\Omega} F_0(t^*)\eta(1 - \eta) \qquad (31)$$

The approximation leading to (31) is strictly valid if $\Omega(2n+1)^2\pi^2$ is very large, which is true if Ω is of order unity. The error that is made by approximating the integral in each term in (29) appears to be very small. However, the errors are added in an infinite sum and there is no easy way to estimate the influence of this. It is possible to arrive at the result in (31) by a more direct approach. The energy eq. (19) can be integrated directly to yield the result in (31) if it is assumed that $\Omega \partial^2\theta/\partial\eta^2 \gg \partial\theta/\partial t$. Notice that this is not necessarily the same as to assume that $\Omega \gg 1$ and that the limiting value of Ω depends on the exact choice of α_1 in the scaling. No serious attempt will be made at investigating the problem in detail here. However, in the light of the numerical solutions later in this article, the approximation seems to be justified for Ω of order unity.

Thus, the instantaneous maximum temperature $\Delta\theta$ in the spatial domain $0 \le \eta \le 1$ will always occur at the center line ($\eta = \tfrac{1}{2}$) and its value is

$$\Delta\theta = \frac{1}{8\Omega} F_0(t^*) \qquad (32)$$

The maximum of the temperature at the center line will therefore occur at the maximum in the reaction rate and with the notation above it is

$$\Delta\theta^* = \frac{1}{8\Omega} F_0|_{\text{max}} \qquad (33)$$

where $F_0|_{\text{max}}$ denotes the maximum value of F_0.

ANALYTICAL SOLUTION FOR A SECOND-ORDER AUTOCATALYTIC KINETIC MODEL

The general solution in (31) can be expressed in closed form for special choices of the kinetic model. In this section, a solution is presented for the second-order autocatalytic model in (6). The time scale for the adiabatic reaction is computed from the reaction rate at $\alpha = 0.5$ [cf. (13)]:

$$\tau = \left\{ \frac{4}{A} \exp\left(\frac{E}{\Delta T_{\text{ad}} R \left[\dfrac{T_0}{\Delta T_{\text{ad}}} + \dfrac{1}{2} \right]} \right) \right\} \qquad (34)$$

Notice that the time scale is independent of the exponent n when $\alpha_1 = 0.5$. The nondimensional form of (6) can after some manipulation be written as

$$\frac{d\alpha}{dt^*} = 4\Gamma^{[1-(\theta_0+\frac{1}{2})/\theta]}\alpha^{2-n}(1-\alpha)^n \qquad (35)$$

where two additional dimensionless parameters (Γ and n) appear. The new parameter Γ is defined by

$$\Gamma = \tfrac{1}{4}A\tau \qquad (36)$$

and it can be interpreted as the ratio between the time scale for an adiabatic reaction and an additional reaction time scale defined by A^{-1}.

The values of the dimensionless parameters for a 3 mm-thick laminate with glass fibers ($V_f = 0.5$) and vinylester (BASF Palatal A-430) and a 5 mm-thick laminate with carbon fibers ($V_f = 0.6$) and epoxy (Fiberite 976) are presented as an example in Table I. The kinetic parameters for the resins have been determined from DSC results with a nonlinear least-squares-fit procedure. The experimental data for the vinylester are from isothermal DSC measurements in our laboratory and the data for the epoxy are from Dusi et al.[9] The material properties of the laminate are shown in Table I.

The dimensionless parameters are of about the same magnitude in the two examples in Table I, but, in general, they can vary within wide limits depending on the thermal and kinetic properties of the material in question. However, in most cases of practical interest (i.e., without high exothermal temperatures), the parameters Ω and θ_0 can be expected to be of order unity.

Specialization of (35) to the case with low exothermal peak temperatures ($\theta \approx \theta_0$) yields

$$\frac{d\alpha}{dt^*} = C_1\alpha^{2-n}(1-\alpha)^n \qquad (37)$$

where the constant C_1 is given by

$$C_1 = 4\Gamma^{-1/2\theta_0} \qquad (38)$$

Equation (37) can be rewritten as

$$\frac{d\alpha}{\alpha^2}\left(\frac{\alpha}{1-\alpha}\right)^n = C_1 dt^* \qquad (39)$$

which can be integrated to

$$\frac{(1/\varepsilon - 1)^{1-n}}{1-n} - \frac{(1/\alpha - 1)^{1-n}}{1-n} = C_1 t^*$$

$$\text{for } n \neq 1 \qquad (40)$$

Table I   Material Properties and the Resulting Dimensionless Parameters for a 3 mm-Thick Glass Fiber–Vinylester Laminate with an Initial Temperature of 35°C and a 5-mm-Thick Carbon Fiber–Epoxy Laminate with an Initial Temperature of 150°C

Parameter	Glass + Vinylester	Carbon + Epoxy	Dimension
L	3	5	[mm]
T_0	308 (35°C)	423 (150°C)	[K]
Porosity	0.5	0.4	[–]
ρ	1890	1580	[kg/m^3]
c	1140	970	[J/kg/K]
λ	0.4	0.7	[W/m/K]
E	$4.3 \cdot 10^4$	$6.9 \cdot 10^4$	[J/mol]
A	$3.7 \cdot 10^4$	$1.2 \cdot 10^5$	[1/s]
n	1.5	1.6	—
H_{tot}	$1.8 \cdot 10^5$	$2.1 \cdot 10^5$	[J/kg]
ΔT_{ad}	158	216	[°C]
τ	65	188	[s]
Ω	1.3	3.3	—
Γ	$6 \cdot 10^5$	$5.5 \cdot 10^5$	—
θ_0	1.9	1.9	—

[a] The thermal conductivity of the composite is computed from the Nielsen rule-of-mixture.[17]

$$\ln\left(\frac{1/\varepsilon - 1}{1/\alpha - 1}\right) = C_1 t^* \quad \text{for } n = 1 \quad (41)$$

The special case with n exactly equal to unity (41) is of little interest and will in the following be left out of the discussion. (The solution below can easily be repeated also for the case $n = 1$.) Equation (40) can be solved for α:

$$\alpha = \frac{1}{1 + [(1/\varepsilon - 1)^{1-n} - (1-n)C_1 t^*]^{1/1-n}} \quad (42)$$

and this solution is plotted in Figure 2 for different values of ε (10^{-6}, 10^{-3}, 10^{-2}, and 0.1). Notice that α depends on the initial value ε, but that this dependence becomes negligible for sufficiently small values of ε when $n > 1$ (see Fig. 2). The dependence on ε is a result of the kinetic model that predicts the zero reaction rate at $\alpha = 0$ and makes it necessary to set the initial value of α to nonzero values to obtain nontrivial solutions. Rearrangement of (42) shows that the dependence on ε is equal to a time shift in the time dependence in α:

$$\alpha = \frac{1}{1 + [(n-1)C_1(t^* - \tau^*)]^{1/1-n}} \quad (43)$$

where the time shift τ^* is given by

$$\tau^* = \frac{(1/\varepsilon - 1)^{1-n}}{(1-n)C_1} \quad (44)$$

Hence, the shape of the curve $\alpha(t^*)$ is independent of ε, although the time at which α attains different values depends on ε. This is also evident in Figure 2 where the horizontal distance between pairs of curves is constant. The solution for α exhibits fundamentally different behavior for $n > 1$ and $n < 1$, respectively. For $n < 1$, the reaction progresses to completion ($\alpha = 1$) for finite times:

$$t^*_{compl} = \frac{(1/\varepsilon - 1)^{1-n}}{C_1(1-n)} \quad \text{for } n < 1 \quad (45)$$

For $n > 1$, the degree of cure will be less than unity for all finite times and the time shift in the solution (τ^*) approaches zero asymptotically as ε approaches zero.

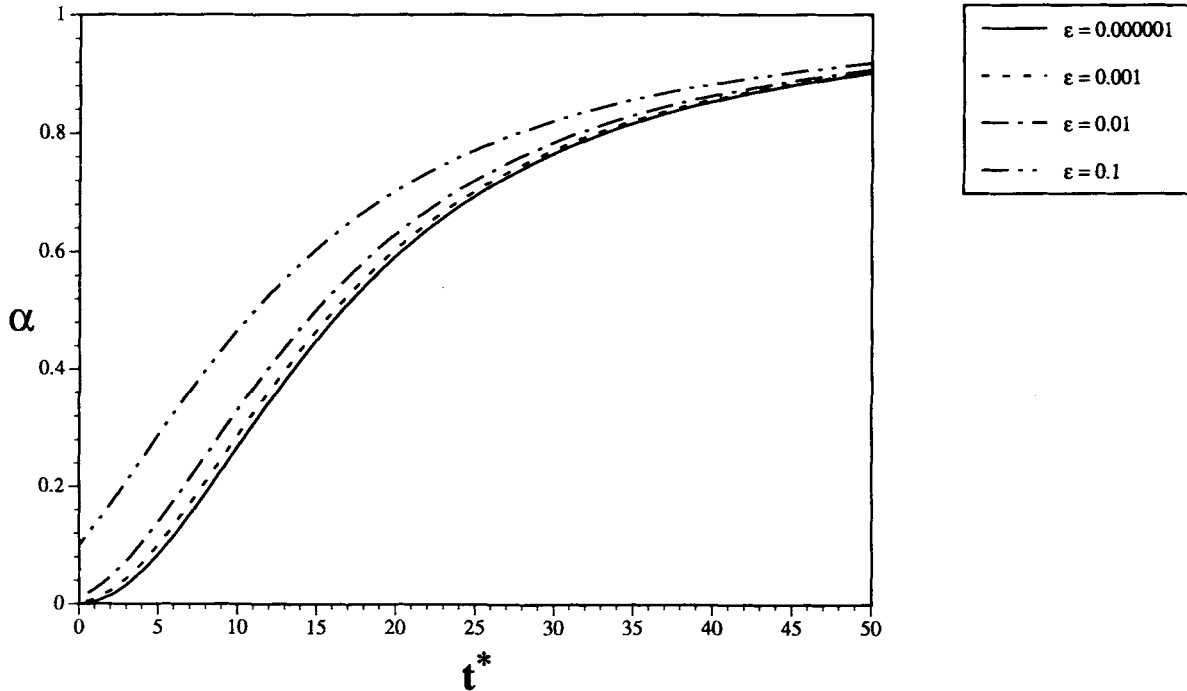The corresponding solution for $d\alpha/dt$ evaluated from (42) or (37) is

Figure 2 Analytical solution for the degree of cure α vs. dimensionless time for four different values of ε. Values for the dimensionless parameters are $\Omega = 1.3$, $\Gamma = 6 \cdot 10^5$, and $\theta_0 = 1.9$.

$$\frac{d\alpha}{dt^*}$$

$$= C_1 \frac{[(1/\varepsilon - 1)^{1-n} - (1 - n)C_1 t^*]^{n/1-n}}{\{1 + [(1/\varepsilon - 1)^{1-n} - (1 - n)C_1 t^*]^{1/1-n}\}^2} \quad (46)$$

The time at which the maximum in $d\alpha/dt^*$ occurs is

$$t_{\text{peak}}^* = \frac{1}{4} \Gamma^{1/2\theta_0} \frac{(1/\varepsilon - 1)^{(1-n)} - \left(\frac{n}{2 - n}\right)^{(1-n)}}{1 - n} \quad (47)$$

and the corresponding value of α is

$$\alpha_{\text{peak}} = 1 - \frac{n}{2} \quad (48)$$

Notice that the time for the maximum t_{peak}^* is practically independent of ε for small values of ε and $n > 1$.

Substitution of $d\alpha/dt^*$ from (46) in (32) makes it possible to evaluate the instantaneous center-line temperature. The solution for the maximum value of the center-line temperature $\Delta\theta^*$ is obtained at the maximum of $d\alpha/dt$ and it takes a remarkably simple form after some algebraic manipulation:

$$\Delta\theta^* = \tfrac{1}{8} n^n m^m \Omega^{-1} \Gamma^{-1/2\theta_0} \quad (49)$$

where $m + n = 2$. Notice that there is no dependence either explicit or implicit on ε. In a practical situation, it is often of interest to keep the maximum temperature below a "target temperature" to minimize the residual stresses in the laminate and to avoid degradation of the matrix material. It is interesting to see how the solution in (49) can be used to predict a suitable processing temperature that will give an acceptable peak temperature for different values of Ω and Γ. To do this, the left-hand side in (49) is set to the target temperature rise $\Delta\theta'$ and the resulting equation for θ_0 is solved:

$$\theta_0 = \frac{1}{2} \frac{\ln \Gamma}{\ln \frac{n^n m^m}{8\Omega\Delta\theta'}} \quad (50)$$

The optimum processing condition map computed from (50) with $\Delta\theta' = 0.01$ is shown in Figure 3 for three different values of Γ. Combinations of θ_0 and Ω below the lines will result in a peak temperature below the target value that was used to compute the lines.

COMPARISON WITH NUMERICAL SOLUTIONS

The analytical solution in the previous section is valid for small exotherm peak temperatures. The exact value of the exotherm temperature for which the solution ceases to be valid is unknown. To investigate this matter in more detail, a series of numerical solutions were computed for various combinations of the dimensionless parameters. The governing equations were integrated with an implicit time-stepping scheme with full nonlinear iteration on each time level.[18,19] The spatial discretization was 50 control volumes across the thickness of the laminate and the initial time step was set to 0.01. The program also has an automatic time-step strategy that tries to keep the maximum change in α between time steps less than 0.001. All computations were performed in single precision, but this caused no significant problem except for a few cases at the very lowest reaction rates where round-off errors appear to influence the result. The initial value of the degree of cure ε was 10^{-5} and the value of n was $\frac{3}{2}$ ($m = \frac{1}{2}$) in all cases.

Figures 4 and 5 show the temporal variation of temperature and degree of cure for three different values of Ω (0.01, 0.1, and 1). The temperature plots in Figure 4 show the gradual transition to adiabatic behavior when Ω decreases. The adiabatic solution in (12) can be rewritten to show that in the adiabatic case

$$\Delta\theta = \alpha \quad (51)$$

The temperature variation for $\Omega = 0.01$ is clearly adiabatic, which can be seen in Figure 6 where the temperature and the corresponding degree of cure are plotted vs. time. Notice the very good agreement with (51) for $\alpha < 0.8$.

The numerical and analytical solutions are compared in Figures 7 and 8 for the case with $\Omega = 1$, $\Gamma = 10^5$, and $\theta_0 = 2.5$. The agreement between the solutions is very good with a maximum relative error in the temperature of about 9%.

The scaling of the peak temperature with the dimensionless parameters Γ and θ_0 is compared to the analytical solution in Figures 9 and 10 and the agreement is found to be excellent for the parameter range investigated.
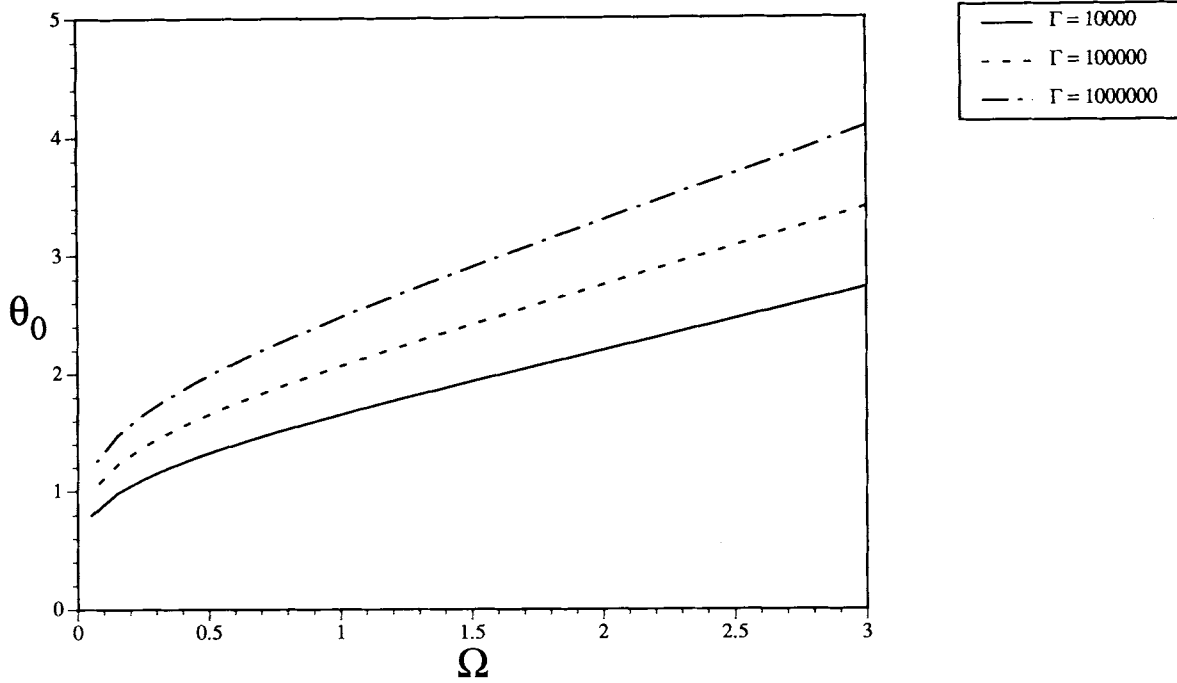
The peak temperature dependence on Ω is inves-

Figure 3 Stability map for three different values of Γ. The target value for the exotherm peak $\Delta\theta'$ is 0.01. Values of Ω and θ_0 above the lines will give a higher exotherm peak than the target value.
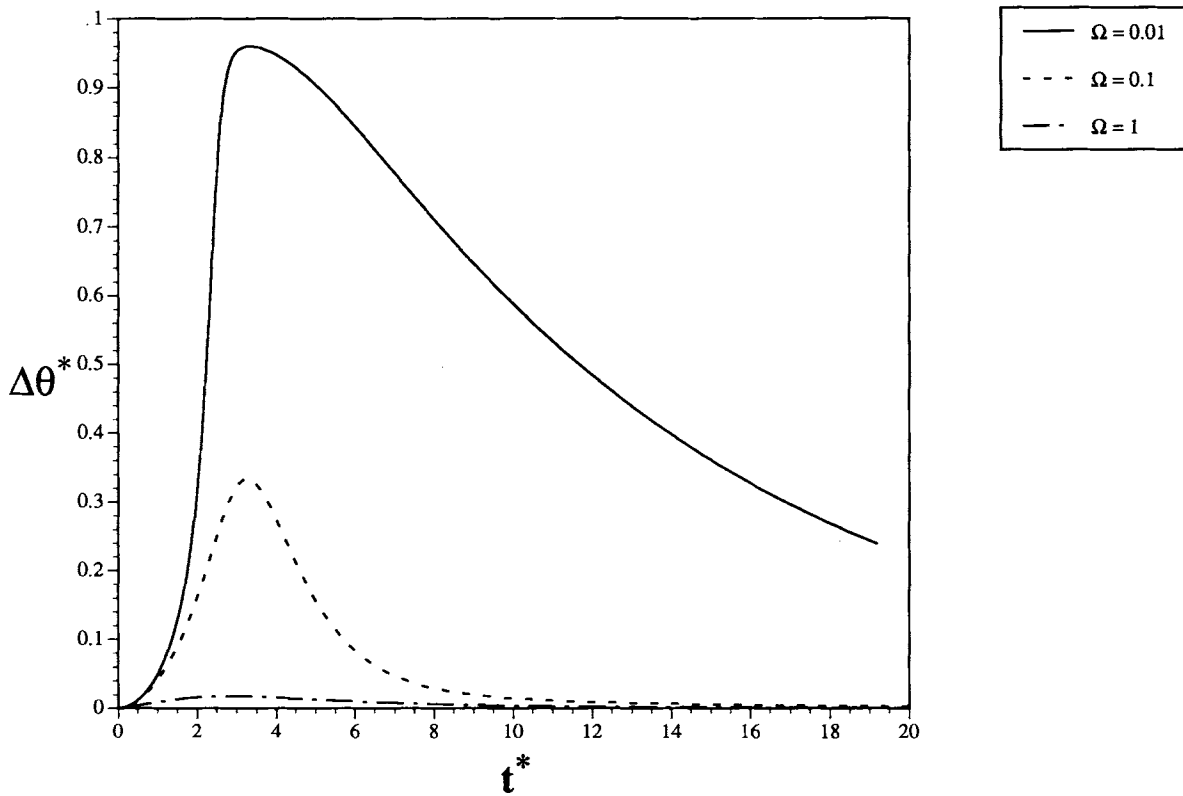

Figure 4 Numerical results for the center-line temperature variation for three different values of Ω ($\Gamma = 10^5$ and $\theta_0 = 2.5$).
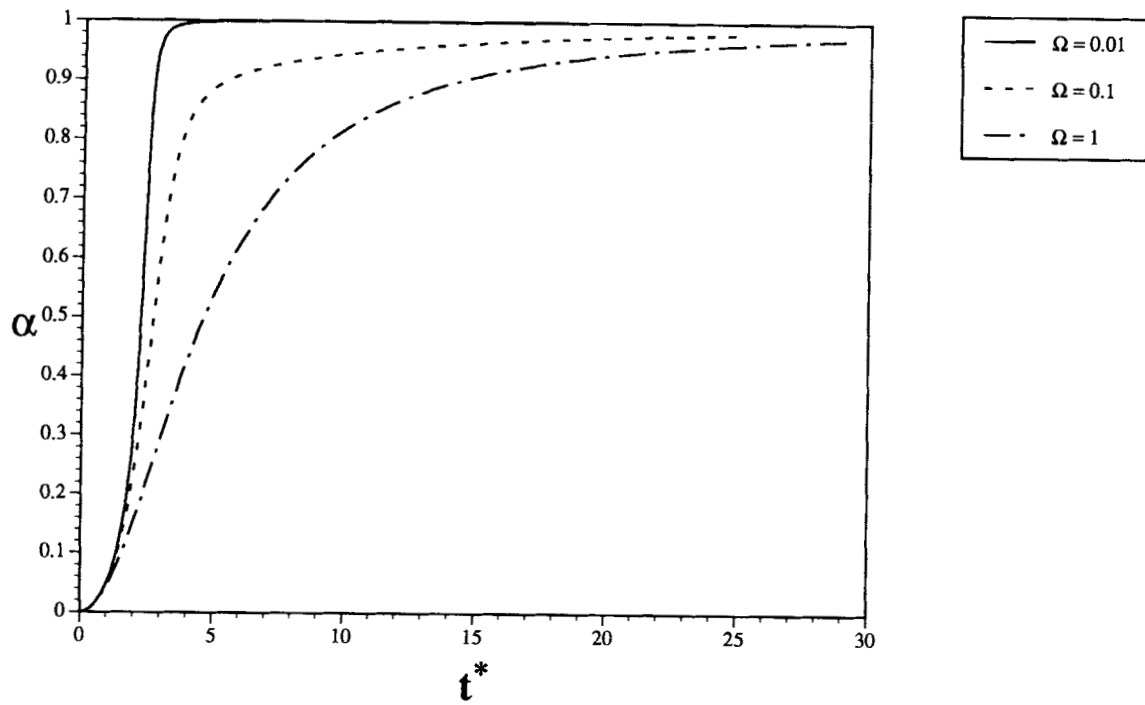
Figure 5 Numerical results for the center-line degree of cure for three different values of Ω ($\Gamma = 10^5$ and $\theta_0 = 2.5$).
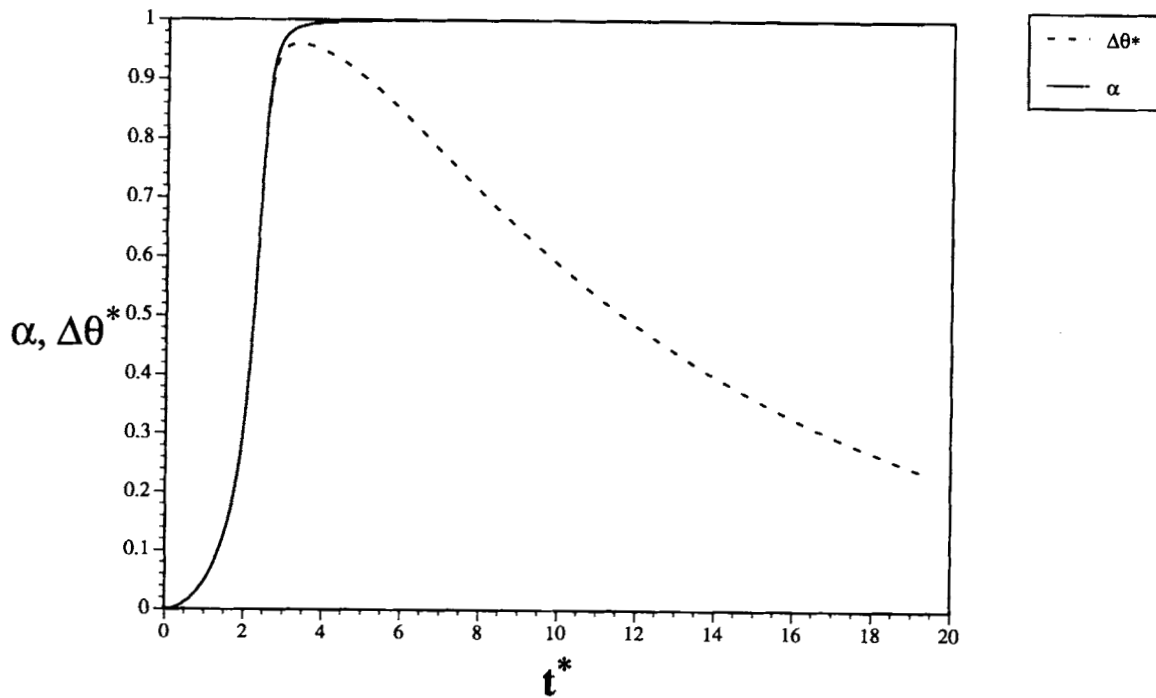
Figure 6 Temperature increase $\Delta\theta^*$ and degree of cure α at the center line for $\Omega = 0.01$ ($\Gamma = 10^5$ and $\theta_0 = 2.5$). Theoretically, $\Delta\theta^* = \alpha$ for an adiabatic cure process.
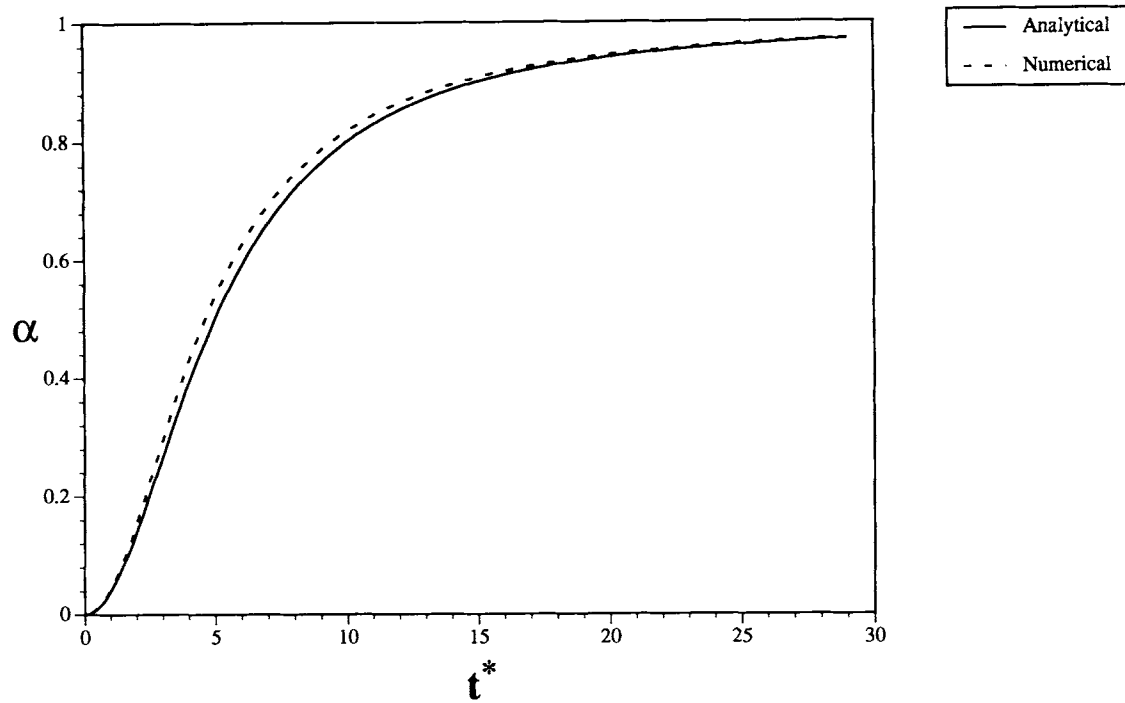
Figure 7 Comparison of the numerical to the analytical solution for the degree of cure with $\Omega = 1$, $\Gamma = 10^5$, and $\theta_0 = 2.5$.
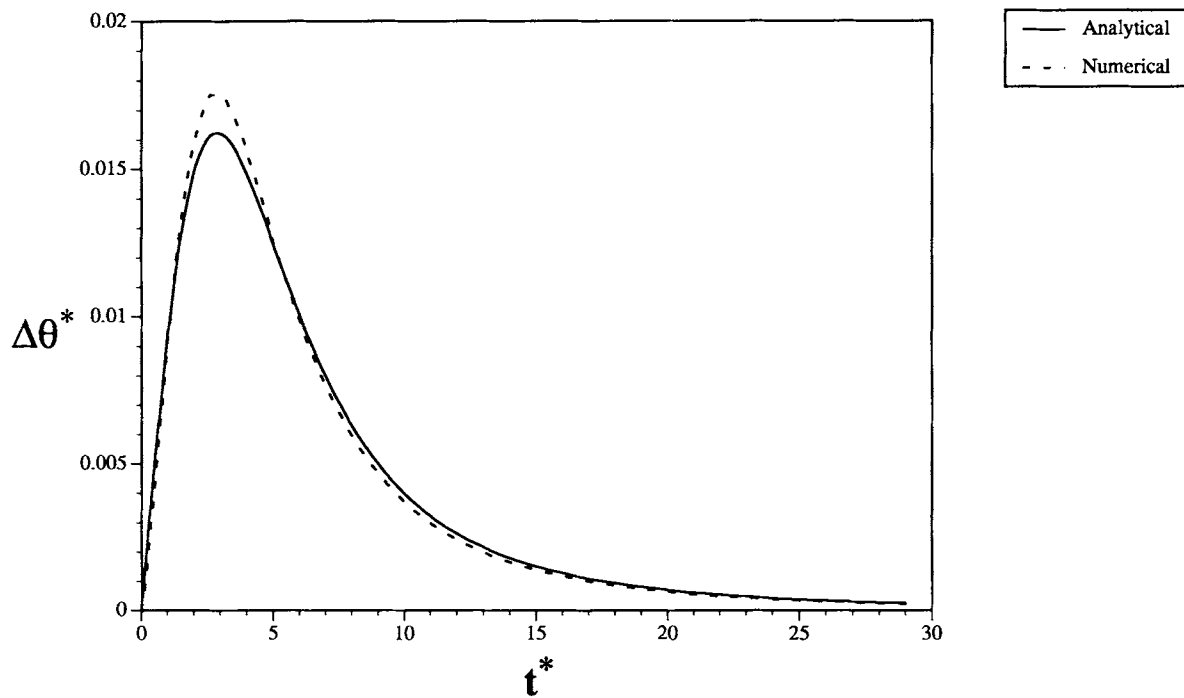
Figure 8 Comparison of the numerical to the analytical solution for the center-line temperature increase with $\Omega = 1$, $\Gamma = 10^5$, and $\theta_0 = 2.5$.
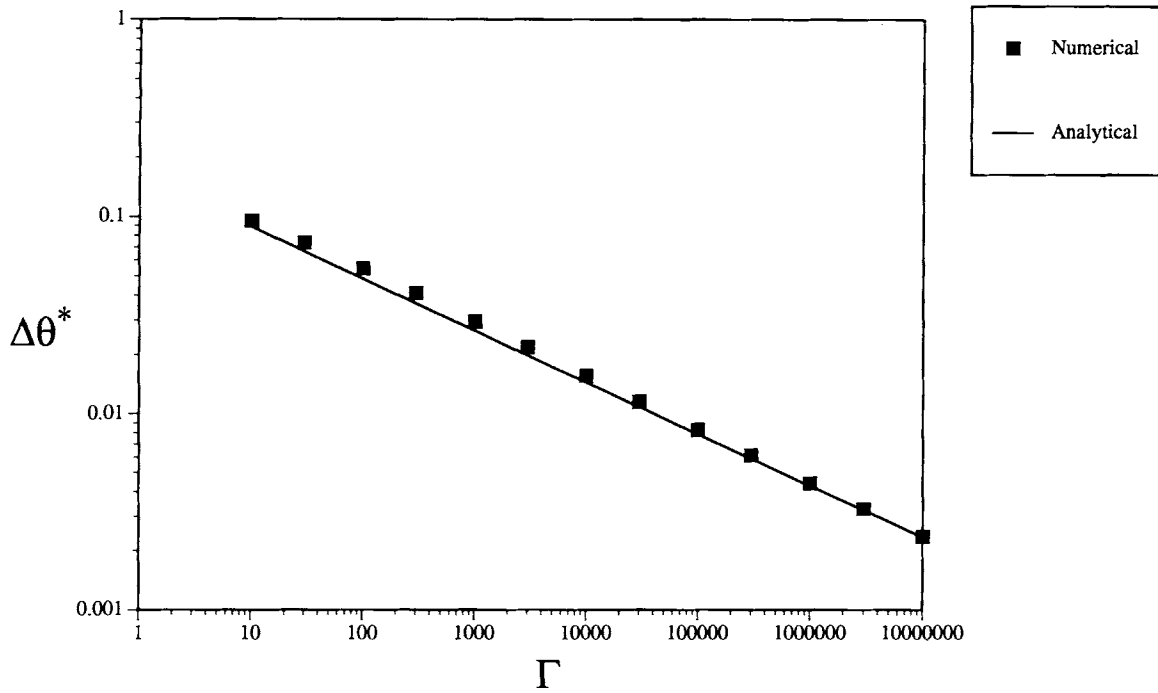
Figure 9 Comparison between numerical and analytical results for the maximum temperature increase at the center line with $\Omega = 1$ and $\theta_0 = 1.9$ vs. Γ.
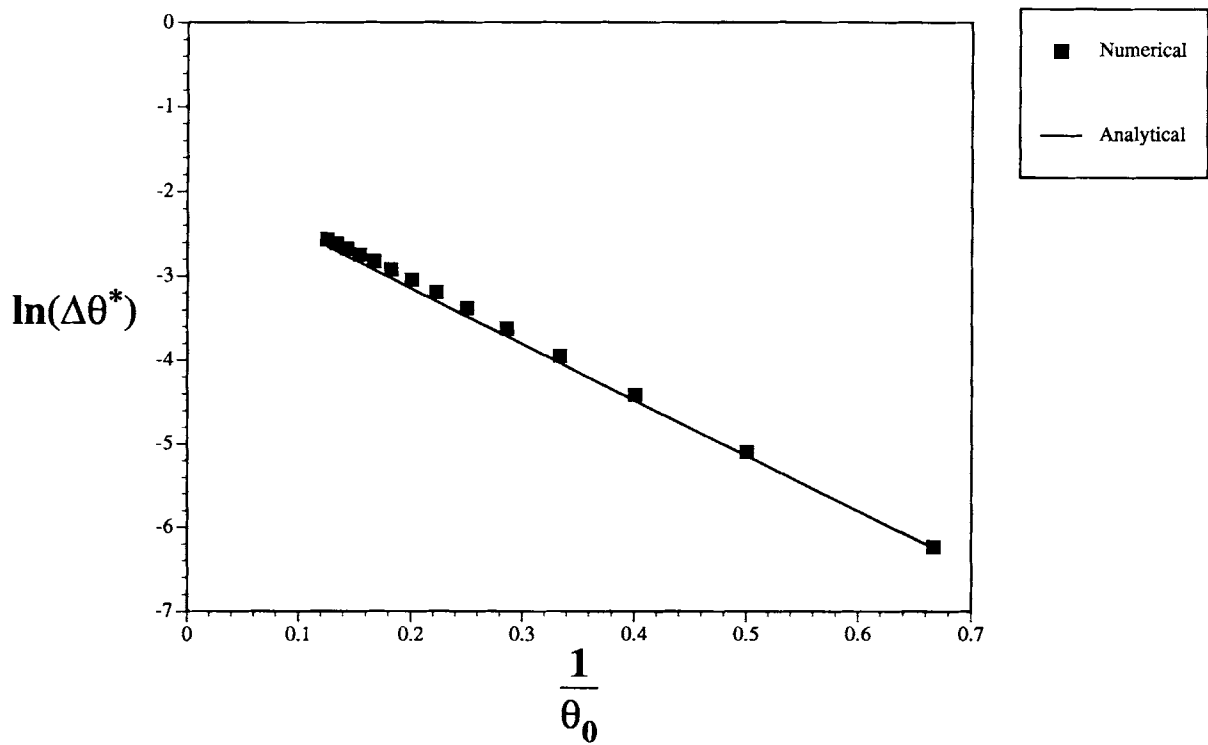

Figure 10 Comparison between numerical and analytical results for ln $\Delta\theta^*$ with $\Omega = 1$ and $\Gamma = 6 \cdot 10^5$ vs. $1/\theta_0$.

tigated in Figure 11 where the results for a wide range of Ω values and two different combinations of θ_0 and Γ are shown. As can be expected, the agreement with the theoretical solution is good at Ω around unity, but it is interesting to notice that the qualitative agreement is good in the whole range of Ω values all the way up to adiabatic conditions (peak temperature = 1).

The analytical solution has also been investigated with respect to the time to peak temperature in (47) (see Fig. 12). The agreement with numerical results is very good also for this aspect of the analytical solution.

The peak temperature from 192 different runs with various combinations of dimensionless parameters is plotted in Figure 13. The abscissa in Figure 13 is the analytical solution for the maximum peak temperature in (49). The theoretical solution (solid line) is also plotted in Figure 13 for comparison. The scatter at low values of the temperature peak are probably a result of round-off errors since this is the region where the approximation should be best. At higher values of the temperature peak, the deviation is a result of nonlinear behavior. Notice that the agreement with the analytical solution is excellent at low exothermal peak values and that it is reasonably good at values of $\Delta\theta$ around 0.1. The

results for $\Omega < 0.5$ in Figure 13 can be seen to deviate slightly from the theoretical solution at intermediate values of the exotherm peak. Some of this deviation probably comes from the approximation of the integral in (29), which becomes less good when $\Omega < 1$.

SUMMARY AND CONCLUSIONS

A general solution for simultaneous heat transfer and chemical reactions in a thermosetting material has been found in the limit of small exothermal temperature peaks. The temperature solution shows that the maximum temperature always occurs at the center line for diffusion Deborah numbers (Ω) of order unity or larger. The peak temperature is proportional to the peak reaction rate and it occurs at the same time that the peak reaction rate occurs.

The kinetic equation is integrated explicitly for the special case with a second-order autocatalytic kinetic model and the result is substituted in the general solution to yield a closed-form solution for the temperature. The analytical solution is compared to numerical results and it is found to be valid with good accuracy as long as the exothermal temperature peak is smaller than about 10% of the adiabatic temperature peak. However, also for higher tem-
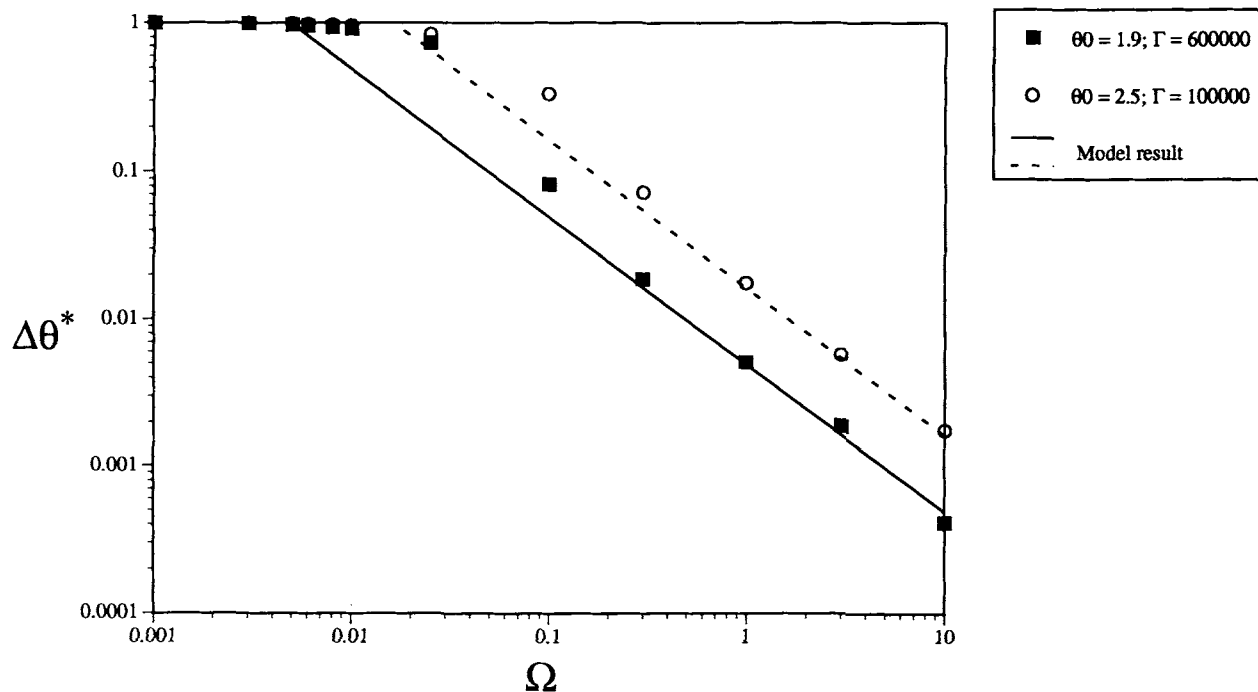

Figure 11   Comparison between the numerical and the analytical solution for the peak temperature vs. Ω with two different combinations of θ_0 and Γ. The lines are the corresponding analytical solutions.
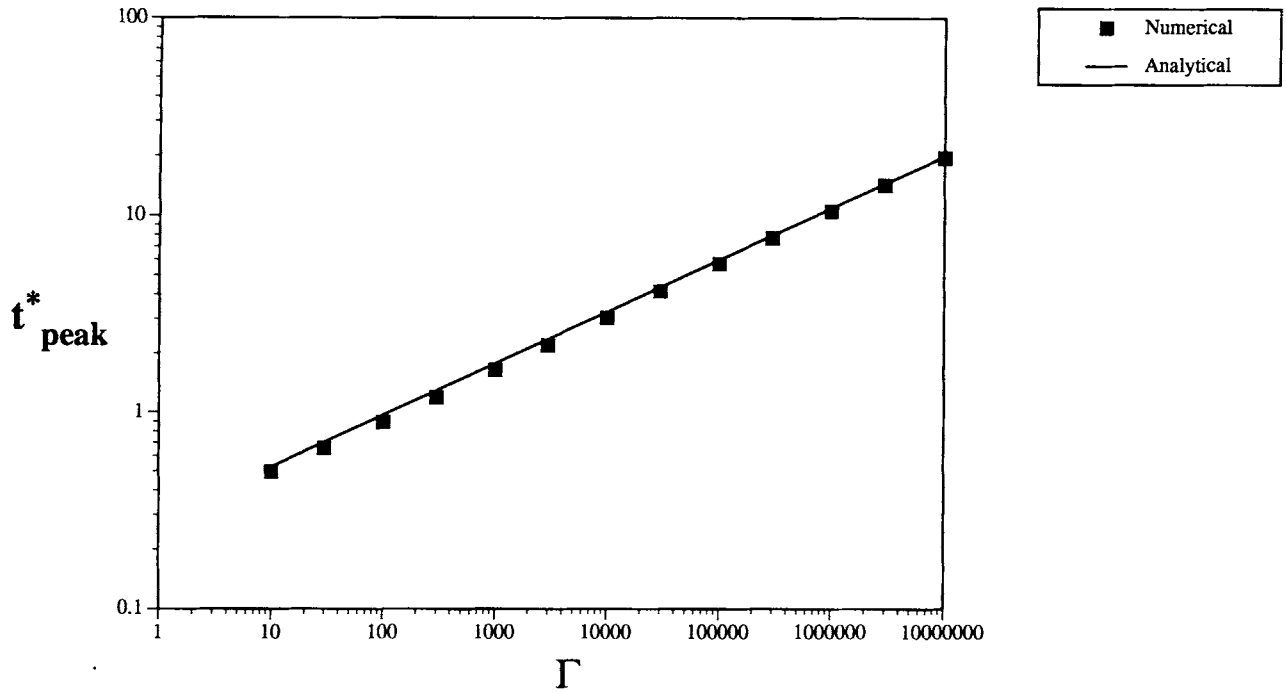
Figure 12 Comparison between the numerical and the analytical solution for the time at which the temperature peak occurs with $\Omega = 1$ and $\theta_0 = 1.9$ vs. Γ.
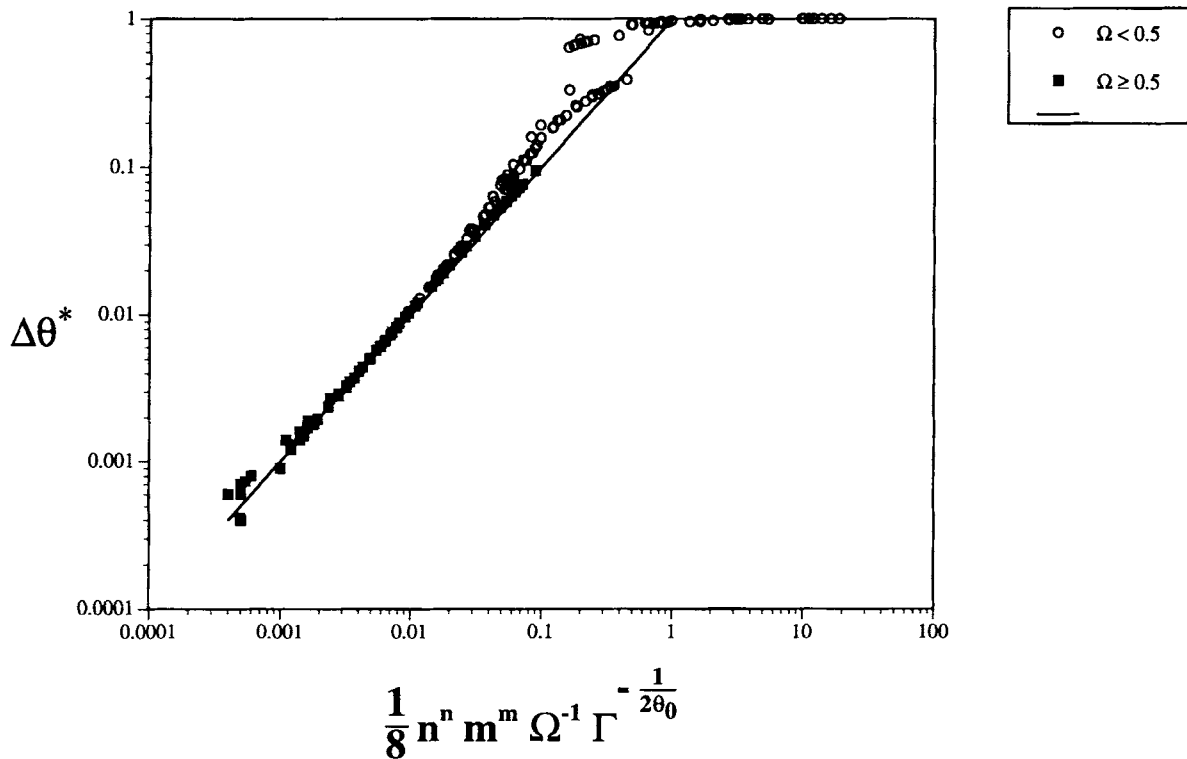

Figure 13 Numerical solutions for a wide range of parameter combinations ($0.001 < \Omega < 30$, $10 < \Gamma < 3.6 \cdot 10^{10}$, and $1.5 < \theta_0 < 8.0$) vs. the theoretical solution for the temperature peak. The analytical solution is plotted for comparison purposes.

perature peaks, the qualitative behavior of the analytical solution is similar to the numerical solution.

The general temperature solution above can be used without a kinetic model since it is valid for all types of time-dependent heat sources. All that is needed to compute the temperature is the time-dependent heat production by the chemical reactions at the processing temperature. Hence, the processing temperature and the formulation of the reacting material can be optimized, with regard to processing time and maximum temperatures, utilizing isothermal DSC measurements. If the computed peak temperature is larger than the desired value, new DSC measurements at lower temperatures are made until the peak temperature is acceptable.

The most critical parameter for the characteristics of the cure process is the diffusion Deborah number (Ω). A prerequisite for high exothermal temperatures appears to be that this parameter is less than unity. Both Ω and the dimensionless processing temperature θ_0 are fundamental parameters in a sense since they do not depend on the particular choice of kinetic model. When a particular kinetic model is introduced, additional dimensionless parameters will appear. The cure behavior for the autocatalytic model above depends less on these additional parameters (Γ and n) than on Ω and θ_0. It is difficult to draw similar conclusions that are valid for general kinetic models. However, it seems likely that the additional parameters in the general case will be less critical than Ω and θ_0 since most models behave qualitatively in the same way as the simple model above.

The isothermal initial condition and the constant wall temperature employed in the present analysis is an approximation of the conditions in real processing situations. The approximation is quite good for a metal mold with water heating but very poor for an unheated composite mold with low thermal diffusivity. Probably the most important deviation from the assumptions in the analysis is that the wall temperature can be time-dependent. Hence, an interesting extension of the present analysis would be to include this feature in the model.

NOTATION

A	frequency factor in kinetic model [s^{-1}]
c	heat capacity [$J/kg\ K$]
C_1	constant in analytical solution
E	activation energy [J/mol]
$f(\alpha, T)$	general expression for the rate of reaction [s^{-1}]
$F(\alpha, \theta)$	dimensionless equivalent of $f(\alpha, T)$
$F_0(t^*)$	reaction rate corresponding to $G(\theta_0, t^*)$
$G(\theta_0, t^*)$	isothermal solution to the kinetic equation
H_{tot}	total heat of reaction [J/kg]
K	rate constant in kinetic model [s^{-1}]
m, n	exponents in kinetic model
q_r	heat production by chemical reactions [W/m^3]
R	universal gas constant (8.314 [$J/mol\ K$])
T	temperature [K]
t	time [s]
t^*	dimensionless time
T_0	initial and boundary temperature [K]
ΔT_{ad}	adiabatic temperature rise (H_{tot}/c) [K]
x	spatial coordinate [m]
α	degree of cure
α_{max}	maximum degree of cure in kinetic model
α_1	characteristic degree of cure
Γ	ratio of two reaction time scales
ε	initial degree of cure
η	dimensionless spatial coordinate
θ	dimensionless temperature
θ_0	dimensionless processing temperature
$\Delta\theta$	center-line temperature rise
$\Delta\theta^*$	maximum value of center-line temperature rise
λ	heat conductivity [$W/m\ K$]
ρ	density [kg/m^3]
τ	characteristic time scale for adiabatic reactions [s]
Ω	diffusion Deborah number

REFERENCES

1. E. Broyer and C. W. Macosko, *AIChE J.,* **22,** 268–276 (1976).
2. J. F. Stevenson, *Polym. Eng. Sci.,* **26,** 746–759 (1986).
3. G. L. Batch and C. W. Macosko, *J. Appl. Polym. Sci.,* **44,** 1711–1729 (1992).
4. M. R. Kamal and M. E. Ryan, *Computer Modeling for Polymer Processing,* Hanser, Munich, 1989, Chap. 2.

5. R. Podgaiz, C. C. Riccardi, and R. J. J. Williams, *Polym. Eng. Sci.*, **32,** 836–840 (1992).

6. J. M. Kenny and A. Trivisano, *Polym. Eng. Sci.*, **31,** 1426–1433 (1991).

7. M. R. Kamal and S. Sourour, *Polym. Eng. Sci.*, **13,** 59–64 (1973).

8. M. E. Ryan and A. Dutta, *Polymer*, **20,** 203–206 (1979).

9. M. R. Dusi, W. I. Lee, P. R. Ciriscioli, and G. S. Springer, *J. Comp. Mater.*, **21,** 243–261 (1987).

10. S. Y. Pusatcioglu, A. L. Fricke, and J. C. Hassler, *J. Appl. Polym. Sci.*, **24,** 937–946 (1979).

11. J. M. Kenny, A. M. Maffezzoli, L. Nicolais, and M. Mazzola, *Compos. Sci. Tech.*, **38,** 339–358 (1990).

12. J. M. Castro, *Polym. Eng. Sci.*, **32,** 715–723 (1992).

13. H. S. Carslaw and J. C. Jaeger, *Conduction of Heat in Solids*, 2nd ed., Oxford University Press, Oxford, 1959.

14. H. E. Adabbo, A. J. Rojas, and R. J. J. Williams, *Polym. Eng. Sci.*, **19,** 835–840 (1979).

15. R. J. J. Williams, A. J. Rojas, J. H. Marciano, and M. M. Ruzzo, *Polym. Plast. Technol. Eng.*, **24,** 243–266 (1985).

16. C. M. Bender and S. A. Orszag, *Advanced Mathematical Methods for Scientists and Engineers*, McGraw-Hill, Singapore, 1978.

17. L. E. Nielsen, *Ind. Eng. Chem. Fundam.*, **13,** 17–20 (1974).

18. S. V. Patankar, *Numerical Heat Transfer and Fluid Flow*, Hemisphere, New York, 1980.

19. B. R. Gebart and L. A. Strömbeck, *Proc. Verbundwerk '92*, Wiesbaden, Germany, 1992.